WALAILAK JOURNAL
http://wjst.wu.ac.th Applied Mathematics

Particle Impaction and Flow through an Infinite Array of Cylinders

Sourabh KHURANA[1,*], Varun GOEL[2], Khushmeet KUMAR[3], Muneesh SETHI[3] and Sourabh KUMAR[4]

[1]*Department of Mechanical Engineering, Chandigarh University, Gharuan 140413, India*
[2]*Department of Mechanical Engineering, National Institute of Technology, Hamirpur 177005, India*
[3]*Department of Mechanical Engineering, Shoolini University, Solan 173212, India*
[4]*Research Scholar at Department of Mechanical Engineering, Indian Institute of Technology, Delhi 110016, India*

([*]Corresponding author's e-mail: sourabhnith@gmail.com)

Received: 29 April 2013, Revised: 21 June 2013, Accepted: 6 February 2014

Abstract

In this paper, the flow field of fluid and trajectory of particle are modeled using FLUENT 12.0. In this software, continuity, momentum and particle flow equations are discretized using the Finite Volume Method (FVM) to calculate the pressure and velocity distribution in the flow domain. A Reynolds number of a value up to 1000 is used to view the flow simulation behind the cylinder, and it is found that at about the value of 100 there is a formation of eddies in the flow. Particle trajectories are calculated using the Lagrangian method. In this model, ash particles of varying diameters are used for capturing over an aluminum cylinder of 50-micron diameter. The particles of lower diameter strictly follow the fluid laminar layers, but as the particle size increases, the trajectory of the particle gets straightened, and it gets impacted on the fiber collector. Finally, the inertial deposition efficiency is calculated and is plotted against the Stoke number. Different cylinder spacing is used, and the effect on capture efficiency is monitored. These results are compared with other theoretical models, and are found to be in excellent co-ordination.

Keywords: Particle capturing, FLUENT, inertial impaction, flow over cylinders.

Nomenclature

C	Spacing between 2 consecutive cylinders.
C_d	Coefficient of drag.
D	Cylinder diameter.
d	Particle diameter.
I	Interception parameter = d / D.
$\overline{p}$	Normalized pressure.
Re_c	Cylinder Reynolds Number.
Re_p	Particle Reynolds Number.
Stk	Stokes Number.
$\overline{t}$	Normalized time.
u, v	Flow velocity in x and y direction respectively.
$\overline{u}, \overline{v}$	Non-dimensional flow velocity in x and y direction respectively.
u_0	Flow velocity.

u_p	Particle velocity.
$\overline{x}, \overline{y}$	Normalized co-ordinates.
x_s	Particle stopping distance.
β	Packing density factor.
γ	Average pressure gradient.
ρ	Flow density.
μ	Flow viscosity.
$\eta_{inertial}$	Inertial impaction efficiency.

Introduction

There is a need for removal of suspended particles from the carrier fluid in many industries. The basic mechanisms by which this particle gets collected are gravity settling, inertial impaction, interception, Brownian diffusion, eddy diffusion, electrostatic precipitation, and thermal precipitation. Different mechanisms have different limitations within which they act efficiently. Inertial impaction and interception are the 2 mechanisms that are dominant in particle collection.

Inertial impaction is characterized by Stokes number, Stk (ratio of the stopping distance of the particle, calculated with an initial velocity equal to that of the upstream air velocity, to the appropriate dimension of the obstacle);

$$Stk = \frac{x_s}{D} = \frac{u_0}{D} = \frac{d^2 \rho u_0}{18 \mu D} \tag{1}$$

The efficiency of impaction can be defined as;

$$\eta_{inertial} = \frac{\text{cross} - \text{sectional area of the fluid stream from which particles are remove}}{\text{cross} - \text{sectional area represented by dimension D, projected upstream}} \tag{2}$$

The inertial deposition of aerosols on cylinders and spheres in cross flow has been studied by various investigators, including Wong and Johnstone [1], Kuwabara [2], Fuchs [3], Davies [4], Strauss [5] and Brauer [6]. Choudhary and Gentry [7] used the method of images to solve steady potential flow past isolated cylinders to study inertial impaction on them. The flow field in the computational domain can be solved by 2 ways: potential flow models and viscous flow models. When compared with experimental results, the efficiency based on viscous flow is quite lower than the efficiency based on potential flow models. Ilias and Douglas [8] provided correlation for inertial deposition for viscous flows past a single cylinder. Israel and Rosner [9] used the term "effective Stokes number", Stk_{eff}, and proposed correlation for the inertial capture efficiency of isolated cylinders and spheres in steady potential flow. Wang [10] used a potential flow model and considered the rebound of particles from cylinders, and Wessel and Righi [11] provided correlations for inertial capture efficiency, impact velocities, particle concentration and angular distributions of particles using the Finite Difference Method (FDM).

Many calculations are present in the literature about the fluid flow past an isolated cylinder. Most of the earlier research is centered on the flow around an isolated cylinder, due to its applicability in many physical problems. Tsiang *et al*. [12], McLaughlin *et al*. [13], Ingham *et al*. [14] and Konstandopoulos *et al*. [15] are some of the investigators who solved the flow problem with an infinite array of fibers in cross flow. Ingham *et al*. [14] applied the Boundary Element Method (BEM) to solve the flow field and compute the particle trajectory. These authors have also taken into account elliptical cylinders in addition to circular cylinders. Konstandopoulos *et al*. [15] applied Method of Images (MOI) to solve the flow

problem and deduced a relationship for the efficiency of capture of particles with a Stokes number. Some investigators have also considered the cylindrical tube banks of heat exchanger to compute the erosion due to the flow of flying ash over those tubes (e.g., Schuh *et al*. [16] and Fan *et al*. [17]). Davies [18] used a Bessel function representation of flow field for $\mathrm{Re}_c = 0.2$, and reported capture efficiency quite lower than that obtained using potential flow methodology. Griffin and Meisen [19] used a steady state solution of Navier-Stokes equations for calculation of capture efficiency of flow past a cylinder for $0.2 < \mathrm{Re}_c < 40$. Brown [20] also solved steady state Navier-Stokes equations for a low range of Reynolds numbers, and presented the equations as linear partial differential equations having Fourier-series solutions. Rao and Faghri [21] studied particle deposition by considering the effect of diffusion of particles on an array of parallel cylinders.

At the start of this century, many researchers chose non-circular cylinders for the purpose of calculation of capture efficiency by arranging them in different arrangements. Non-circular cylinders offer more advantage over circular cylinders, as they have more surface to volume ratio as compared to circular ones. Raynor [22] developed correlation of fiber collection efficiency for elliptical fibers for different values of particle diameter, solidity and aspect ratio. Chen *et al*. [23], Ming and Liu [24] and Zhu *et al*. [25] conducted numerical analysis of flow past a rectangular cylinder and calculated collection efficiency by varying cylinder aspect ratio, particle diameter and packing density of fibers.

The present paper is centered on the study of inertial impaction on circular cylinder arrays by solving the Navier-Stokes equation for viscous flow. The pressure drop across the cylinder and variation of different flow parameters are monitored with the variation of cylinder spacing. Then, inertial impaction efficiency is calculated using the above formula.

Mathematical model

The fibrous filter model consists of an array of circular cylindrical fibers as shown in **Figure 1**. Flow is assumed to be steady, uniform, incompressible, irrotational, laminar, and Newtonian. For the cylinder fibers, no slip condition is applied. Different equations are solved in between the line of symmetry for obtaining the solution, as on the other side of the symmetric line the result of the flow field will be a symmetrical inversion of the computed result. A packing density factor is used in the work, defined as;

$$\beta = \frac{\pi}{4}\left(\frac{D}{C}\right)^2 \tag{3}$$

where D is the cylinder diameter and C is the cylinder spacing.

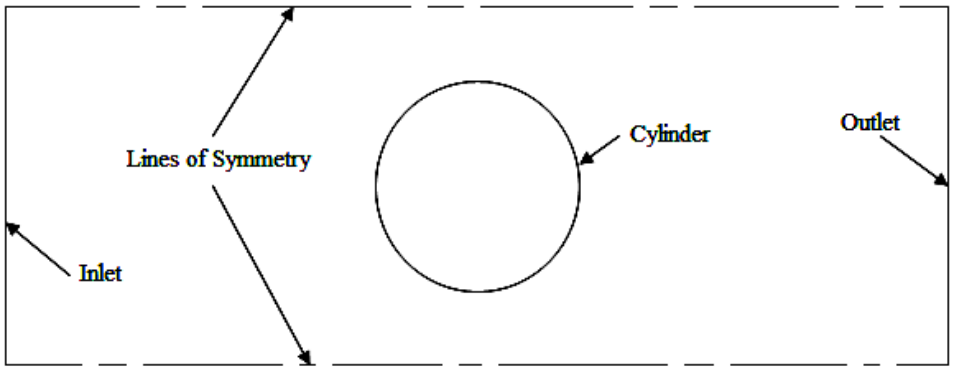

Figure 1 Schematic diagram of a single cylinder in the flow domain.

The governing equations for two-dimensional incompressible flow with no body forces are the continuity equation and the Navier-Stokes equation in 2 directions (Schlichting, [26]). In rectangular co-ordinates, the non-dimensional forms of these equations are;

$$\frac{\partial \bar{u}}{\partial \bar{x}} + \frac{\partial \bar{v}}{\partial \bar{y}} = 0 \tag{4}$$

$$\frac{\partial \bar{u}}{\partial \bar{t}} + \bar{u}\frac{\partial \bar{u}}{\partial \bar{x}} + \bar{v}\frac{\partial \bar{u}}{\partial \bar{y}} = -\frac{\partial \bar{p}}{\partial \bar{x}} + \frac{2}{\mathrm{Re}_c}\left(\frac{\partial^2 \bar{u}}{\partial \bar{x}^2} + \frac{\partial^2 \bar{u}}{\partial \bar{y}^2}\right) \tag{5}$$

$$\frac{\partial \bar{v}}{\partial \bar{t}} + \bar{u}\frac{\partial \bar{v}}{\partial \bar{x}} + \bar{v}\frac{\partial \bar{v}}{\partial \bar{y}} = -\frac{\partial \bar{p}}{\partial \bar{y}} + \frac{2}{\mathrm{Re}_c}\left(\frac{\partial^2 \bar{v}}{\partial \bar{x}^2} + \frac{\partial^2 \bar{v}}{\partial \bar{y}^2}\right) \tag{6}$$

However, there are 2 modifications in Eqs. (4), (5) and (6) for 2 different type of flows, namely viscous flow and potential flow. For viscous flow $\mathrm{Re}_c << 1$, it is assumed that viscous flow is the only dominating force, and all inertial terms in the equation are neglected. In the potential flow $\mathrm{Re}_c \to \infty$, all inertial forces are considered dominating, and viscous forces are neglected (Lamb, [27]). The approximations are;

Viscous flow

$$\bar{u} = \frac{\ln\sqrt{\bar{x}^2 + \bar{y}^2} + \dfrac{\left(\bar{x}^2 + \bar{y}^2\right)\left(\bar{y}^2 - \bar{x}^2\right)}{\left(\bar{x}^2 + \bar{y}^2\right)^2}}{2.002 - \ln \mathrm{Re}_c} \tag{7}$$

$$\bar{v} = -\frac{\left(\bar{x}^2 + \bar{y}^2 - 1\right)\bar{x}\bar{y}}{\left(2.002 - \ln \mathrm{Re}_c\right)\left(\bar{x}^2 + \bar{y}^2\right)} \tag{8}$$

Potential flow

$$\bar{u} = 1 + \frac{\left(\bar{y}^2 - \bar{x}^2\right)}{\left(\bar{x}^2 + \bar{y}^2\right)^2} \tag{9}$$

$$\bar{v} = -\frac{2\bar{x}\bar{y}}{\left(\bar{x}^2 + \bar{y}^2\right)} \tag{10}$$

To obtain the solution of particle trajectory, the above four conditions are used as boundary conditions in the particle trajectory equation. However, the full solution of the Navier-Stokes equation is

required for tracing the particle trajectory. In this work, the dimensional form of governing equations is used with these boundary conditions for the solution of Navier-Stokes equation:

Inlet

Velocity inlet condition is given at the entrance, only x - direction velocity is specified, and y - direction velocity is assumed as zero.

Outlet

Outflow condition is given at the exit, although the velocity normal to the flow i.e. in y - direction is assumed as zero. The value of other variables is the same as calculated by the software.

Upper and Lower Boundary

These are the symmetry boundaries of the flow domain, so symmetry condition is applied to these boundaries.

$$\frac{\partial u}{\partial y} = 0, v = 0 \tag{11}$$

Cylinder fiber surface

Fiber surface is assumed to be stationary and irrotational with no slip condition. At the cylinder surface, the flow velocities are zero.

$$u = 0, v = 0 \tag{12}$$

These boundary conditions are not complete to obtain the full solution of governing equations; for that, the concept of Patankar *et al*. [28] is used. The pressure p decreases in the direction of the main flow; this can be expressed as;

$$p(x, y) = P(x, y) - \gamma x \tag{13}$$

where γ is the average pressure gradient in the direction of the main flow. Using the above boundary conditions and assumptions in the governing equations, the following solution is obtained.

$$\rho\left(u\frac{\partial u}{\partial x} + v\frac{\partial u}{\partial y}\right) = \gamma - \frac{\partial P}{\partial x} + \mu\left(\frac{\partial^2 u}{\partial x^2} + \frac{\partial^2 u}{\partial y^2}\right) \tag{14}$$

$$\rho\left(u\frac{\partial v}{\partial x} + v\frac{\partial v}{\partial y}\right) = -\frac{\partial P}{\partial x} + \mu\left(\frac{\partial^2 v}{\partial x^2} + \frac{\partial^2 v}{\partial y^2}\right) \tag{15}$$

Now, the above equations have only 3 variables u, v and P. These equations are solved by the algorithm of Patankar *et al*. [28].

Numerical simulation

The Finite Volume Method (FVM), in combination with Semi-Implicit Method for Pressure Linked Equations (SIMPLE), is used to solve the governing equations. The control volume approach is used to solve the problem, and a staggered grid is considered so that pressure is computed at the centre of the control volume while the velocity components are computed at the faces of the control volume. A

triangular mesh is used in this work, with very fine mesh around the cylinder. **Figure 2** shows the zoomed view of the meshed structure of the flow domain used in this work. Tests are carried out to check the mesh independence of the results at each node. Errors of the order of 10^{-3} are used in the calculation of residuals in the work.

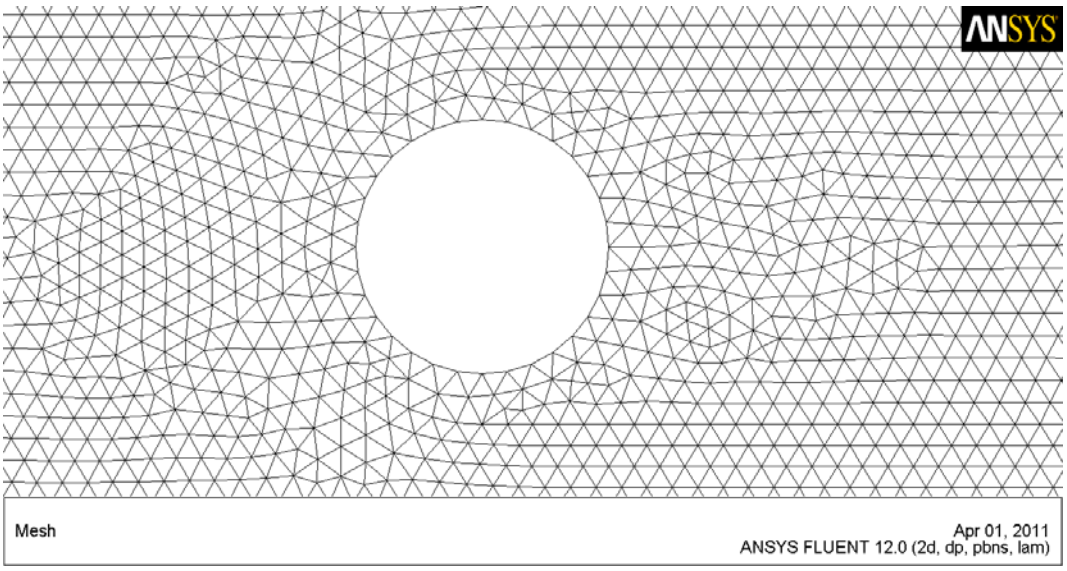

Figure 2 Mesh structure of flow domain.

The Tri-Diagonal Matrix Algorithm (TDMA) is applied to solve the flow problem. A general two-dimensional discretized equation for the flow problem is;

$$a_P\phi_P = a_W\phi_W + a_E\phi_E + a_S\phi_S + a_N\phi_N + b \tag{16}$$

where a_p is the coefficient of variable ϕ_p at node P in the mesh shown in **Figure 3**, and b is the source term. To solve the above equation along the N-S line, the equation is rearranged in the form;

$$-a_N\phi_N + a_P\phi_P - a_S\phi_S = a_W\phi_W + a_E\phi_E + b \tag{17}$$

Now this equation can be written as;

$$-\alpha_j\phi_{j+1} + D_j\phi_j - \beta_j\phi_{j-1} = C_j \tag{18}$$

where $\alpha_j = a_N, \beta_j = a_S, D_j = a_P, C_j = a_W\phi_W + a_E\phi_E + b$. In this case, ϕ_W and ϕ_E are assumed to be zero in the first iteration, and in the further iterations, its value is taken as the value coming from the previous run of calculation. The solution of the flow domain can be calculated explicitly using values j = 2, 3, 4,…, n. When calculation for current column is completed, the next N-S line is taken for the calculation.

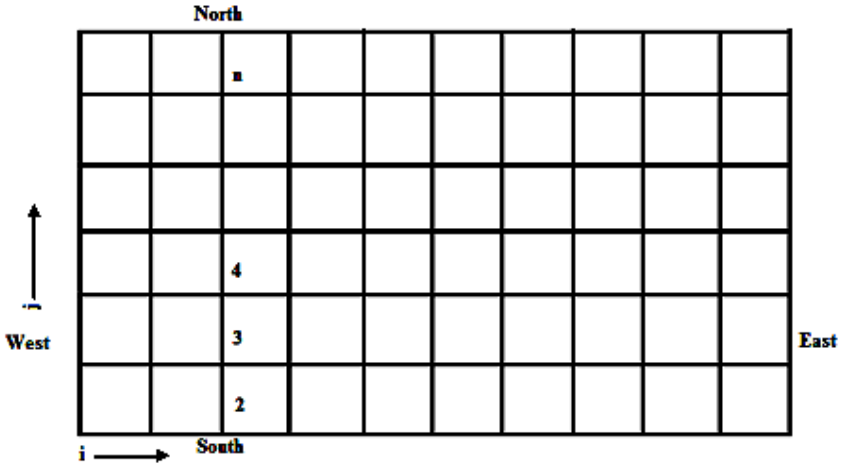

Figure 3 Application of TDMA in two dimensional domain.

Particle impaction

When a gas stream containing suspended particles flows across a circular cylinder, it tends to flow around it. However, larger particles tend to continue in the straight path, because of its inertia. They may strike on the cylinder surface and gets collected. For computation of the collection efficiency, the equation of motion must be solved with the fluid flow model. The equations of motion of particles in a non-dimensional form in 2 dimensions are (Strauss, [5]);

$$\frac{48Stk}{C_d \operatorname{Re}_p}\frac{d^2\bar{x}}{d\bar{t}^2}+\frac{d\bar{x}}{d\bar{t}}-p\bar{x}=0 \tag{19}$$

$$\frac{48Stk}{C_d \operatorname{Re}_p}\frac{d^2\bar{y}}{d\bar{t}^2}+\frac{d\bar{y}}{d\bar{t}}-q\bar{y}=0 \tag{20}$$

where Stk is the Stokes Number calculated from Eq. (1), p and q are the constants, and C_d is the coefficient of drag of the particle;

$$C_d = A_1+\frac{A_2}{\operatorname{Re}_p}+\frac{A_3}{\operatorname{Re}_p^2} \tag{21}$$

where A_i's are the constants and;

$$\operatorname{Re}_p=\frac{d_p\,|u-u_p|\,\rho}{\mu} \tag{22}$$

The solution to Eq. (19) is given by;

$$\bar{x} = Ae^{\lambda_1 t} + Be^{\lambda_2 t} \tag{23}$$

where λ_1 and λ_2 are the solution of the characteristic equation;

$$Stk\lambda^2 + \lambda + p = 0 \tag{24}$$

and

$$\lambda = -\frac{-1 \pm \sqrt{1 - 4pStk}}{2Stk} \tag{25}$$

Similarly, the solution for Eq. (20) can be calculated and finally particle trajectory can be traced in the flow domain. A particle in the gas stream will be captured when its trajectory falls on the cylinder surface. In this paper, the effect of particle rebound from the surface of the cylinder after it strikes the cylinder has not been taken into account.

Results and discussion

In this paper, fiber collection efficiency and flow field variables are calculated at different Reynolds Numbers, Stokes Numbers, and cylinder packing density factors. A cylinder diameter of 50 microns and varying values of particle diameter and flow velocity depending upon Stokes Number is used in this work. Representative velocity profiles close to the cylinder for 7 different values of Reynolds Number of 10, 50, 100, 250, 500, 750 and 1000 are shown in **Figure 4**. The strouhal number calculated here is 0.21. It can be observed in the following figures that vortex shedding starts at around a Reynolds number of 100 and its magnitude increases continuously as the Reynolds number increases. Due to formation of this vortex, there are sudden changes in some flow quantities, like length and width of the wake region, while vorticity and pressure distributions on the surface of cylinder are quite unaffected.

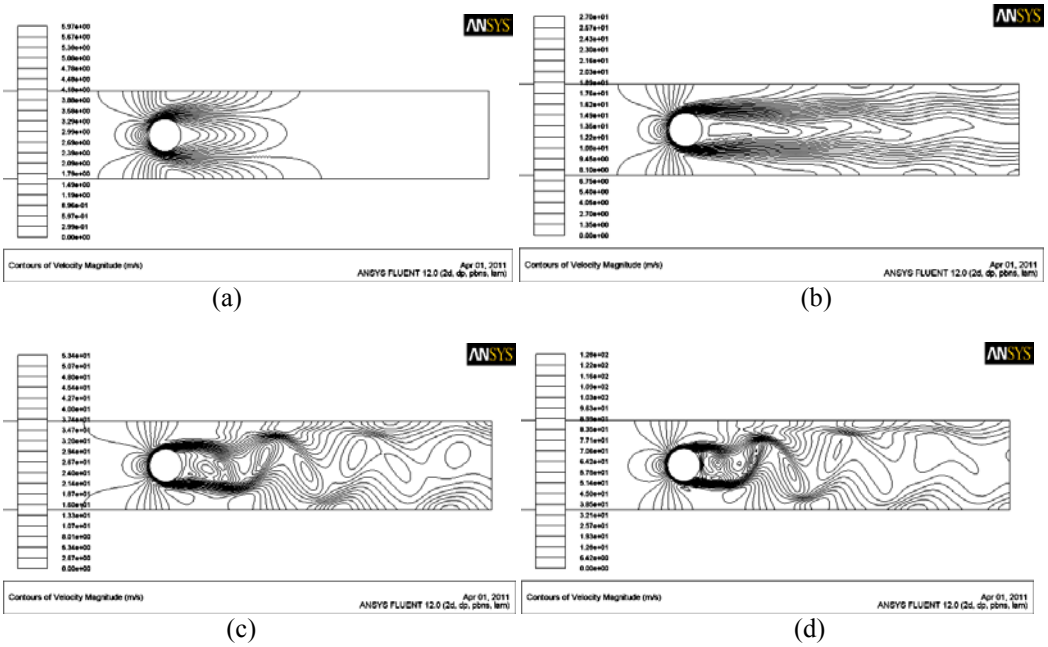

(a) (b)

(c) (d)

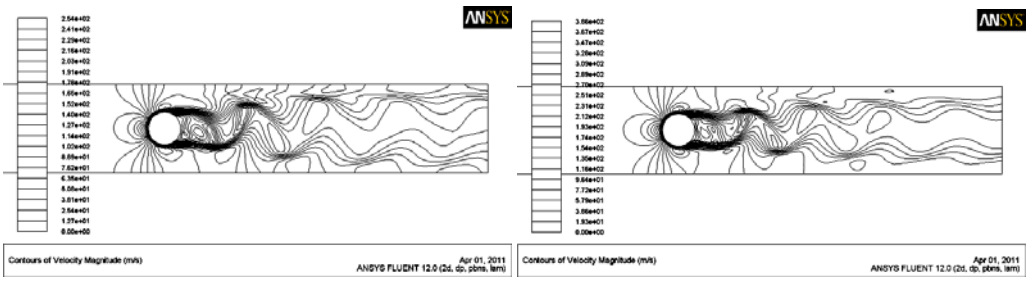

(e) (f)

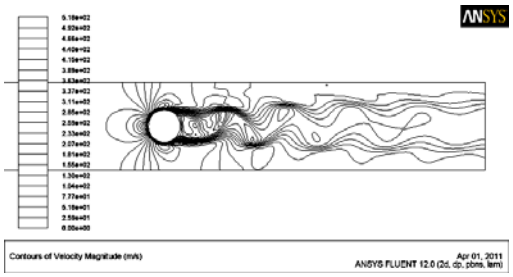

(g)

Figure 4 Velocity Profiles at different Reynolds Numbers. (a) Re = 10, (b) Re = 50, (c) Re = 100, (d) Re = 250, (e) Re = 500, (f) Re = 750 and (g) Re = 1000.

Table 1 shows the different values of drag coefficients of the cylinder at different values of Reynolds Number. From this table, it can be concluded that the drag coefficient for every value of Reynolds number in the case of $\beta = 0.01$ is lower than that of $\beta = 0.11$; this is because, in the later case, the cylinders are closely packed, so there is a sudden change in the flow comparative to the former case. It can also be concluded from the table that as the Reynolds number increases, the drag coefficient decreases. The reason is that as the velocity of flow increases and the flow adjusts itself quite earlier than at a lower Reynolds number.

Table 1 Comparison of drag coefficient.

Reynolds number	**Drag coefficient**	
	$\beta = 0.01$	**$\beta = 0.11$**
4.41	0.0004628	0.0006726
8.82	0.0002488	0.0003971
13.23	0.0001842	0.0003074
17.64	0.0001557	0.0002615
22.05	0.0001406	0.0002332
26.46	0.0001299	0.0002139

Comparisons are made at constant interception parameter I = 0.05, and collection efficiency is computed at each Stokes number by varying the Reynolds number. In **Figure 5** the packing density factor of 0.01 is used, while in **Figure 6**, the factor of 0.11 is used.

The main aspects of the 4 theoretical models are as follows:

1) Choudhary and Gentry [7]. The flow field around 2 cylinders are solved using Method of Images with the assumption of potential flow. The flow is assumed inviscid and collection efficiency is computed using Langmuir's method.

2) Davies and Peetz [29]. The flow field around one fiber is computed using a viscous flow approach at Re = 0.2 and collection efficiency is calculated using Langmuir's method.

3) Harrop and Stenhouse [30]. They used cellular model to calculate the creeping motion around the cylinder. However, collection efficiency is calculated by the same method as above.

4) Mc Laughlin *et al*. [13]. These authors used FEM for the solution of Navier-Stokes equation for the solution of the flow field. For the calculation of collection efficiency, they integrated the total number of intercepted particles on the cylinder surface.

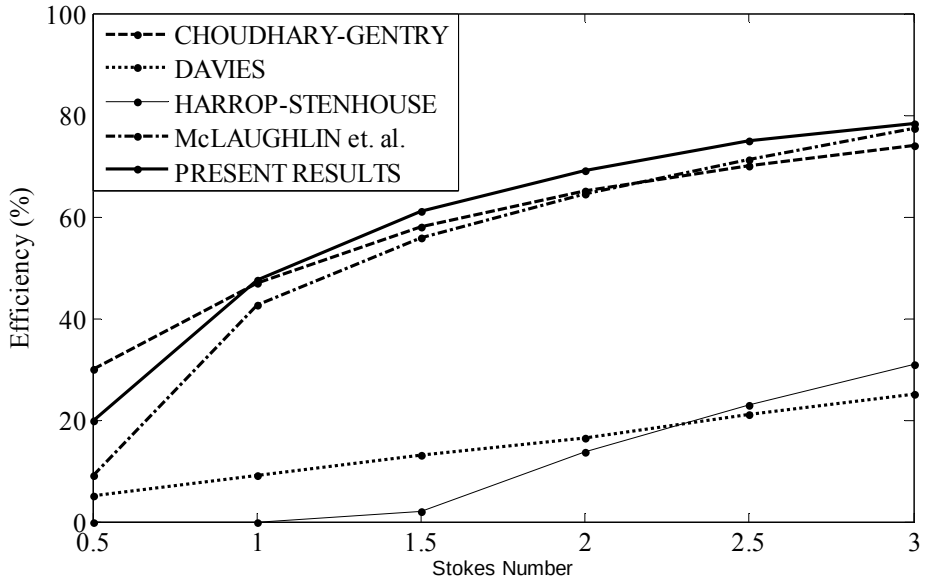

Figure 5 Comparison of fiber collection efficiency for β = 0.01.

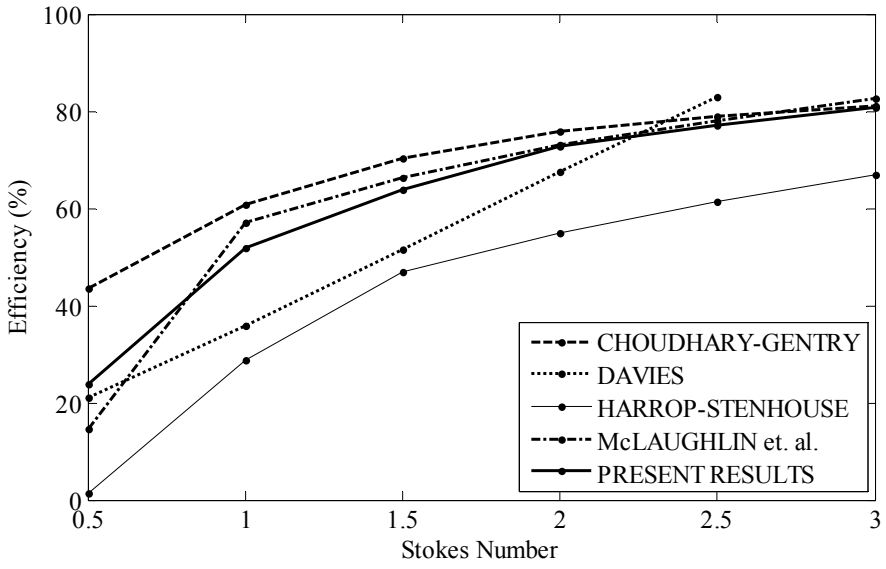

Figure 6 Comparison of fiber collection efficiency for $\beta = 0.11$.

The present model gives a result closer to those of Choudhary and Gentry [7] and McLaughlin *et al*. [13]. This is expected, as the Reynolds number increases with the Stokes number, and the flow is assumed as potential flow. The result of Harrop and Stenhouse are quite low, at a low packing density factor. This is because they have taken a very low Reynolds number, and so their results are accurate in the lower Stokes range. This is the reason for the lower efficiency of the result of Davies. Therefore, the model used in the present paper produces a more accurate result than previously developed models.

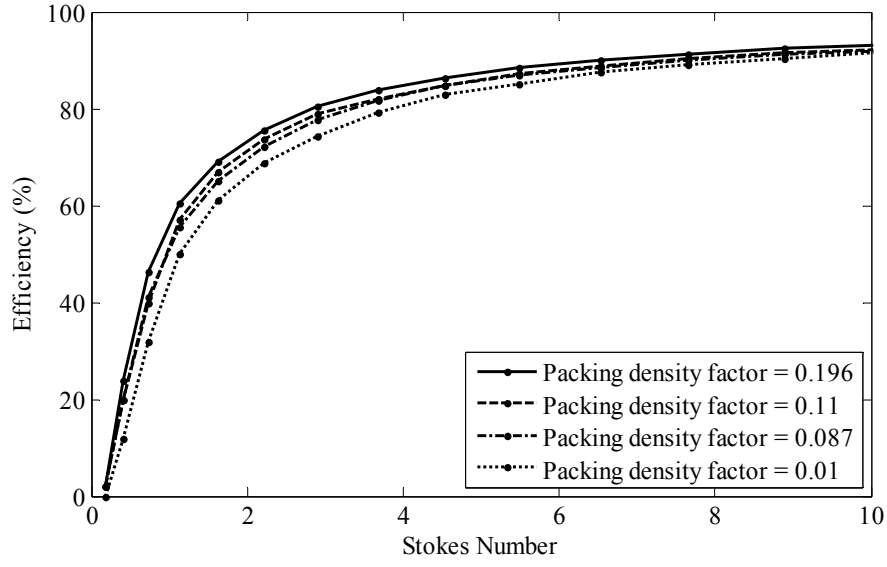

Figure 7 Comparison of collection efficiency at different values of packing density factor.

In **Figure 7** there is a comparison of collection efficiency at values of β = 0.196, 0.01, 0.087 and 0.11. It can be found from the figure that as the Stokes number increases, the value of collection efficiency decreases with a decreasing value of packing density factor (β). The Reynolds number for this computation is Re_c = 10. This is due to the reason that as β increases, the fibers are closer to each other than at lower value of β, and when the fibers are close to each other, there are sudden changes in the flow direction. The particles of smaller diameter can follow that sudden change up to certain extent, but the particles with larger diameters cannot follow that change, and they get impacted on the cylinder.

Conclusions

The inertial deposition model is developed using the software FLUENT 12.0. The collection efficiency of ash on an array of cylinders is computed using the software for a wide range of Stokes numbers, Reynolds numbers and packing density factors. Computed inertial impaction efficiency is found to be in good agreement with the previously developed deposition models. There is reasonable improvement in the results obtained when it is compared with some available classical models.

References

[1] JD Wong and HF Johnstone. *Engineering Experimental Station*. University of Illinois, Technical Report Number 11, 1953.
[2] S Kuwabara. The forces experienced by randomly distributed circular cylinders or sphere in a viscous flow at small Reynolds number. *J. Phys. Soc. Japan* 1959; **14**, 527-32.
[3] NA Fuchs. *The Mechanics of Aerosols*. 6th ed. Pergamon, New York, 1964.
[4] CN Davies. Deposition of aerosols from turbulent flows through pipes. *Proc. Roy. Soc.* 1965; **289**, 235-46.
[5] W Strauss. *Industrial Gas Cleaning*. 2nd ed. Pergamon, New York, 1975.
[6] H Brauer. *Movement of Single Particles in Various Flow Fields. In*: AS Majumder and RA Mashelkar (eds.). Advances in Transport Process, 1982, p. 1-353.
[7] KR Choudhary and JW Gentry. A model for particle collection with potential flow between two parallel cylinders. *Can. J. Chem. Eng.* 1977; **55**, 403-7.
[8] S Ilias and PL Douglas. Inertial impaction of aerosol particles on cylinders at intermediate and high Reynolds numbers. *Chem. Eng. Sci.* 1989; **44**, 81-99.
[9] R Israel and DE Rosner. Use of a generalized Stokes number to determine the aerodynamic capture efficiency of non-Stokesian particles from a compressible gas flow. *Aerosol Sci. Tech.* 1983; **9**, 29-60.
[10] HC Wang. Theoretical adhesion efficiency for particles impacting a cylinder at high Reynolds number. *J. Aerosol Sci.* 1986; **17**, 827-37.
[11] RA Wessel and J Righi. Generalized correlations for inertial impaction of particles on a circular cylinder. *Aerosol Sci. Tech.* 1988; **9**, 29-60.
[12] C Tsiang, CS Wang and C Tien. Dynamics of particle deposition on model fiber filters. *Chem. Eng. Sci.* 1982; **37**, 1661-73.
[13] C McLaughlin, P McComber and A Gakwaya. Numerical calculation of particle collection by a row of cylinders in a viscous fluid. *Can. J. Chem. Eng.* 1986; **64**, 205-10.
[14] DB Ingham, ML Hildyard and PJ Heggs. The particle collection efficiency of a cascade of cylinders. *Can. J. Chem. Eng.* 1989; **67**, 545-53.
[15] AG Konstandopoulos, MJ Labowsky and DE Rosner. Inertial deposition of particles from potential flows past cylinder arrays. *J. Aerosol Sci.* 1993; **24**, 471-83.
[16] MJ Schuh, CA Schuler and JAC Humphrey. Numerical calculation of particle-laden gas flows past tubes. *AIChE J.* 1989; **35**, 466-80.
[17] J Fan, D Zhou, J Jin and K Cen. Numerical calculation of tube bundles erosion by turbulent particle-laden gas flows. *Chem. Eng. Comm*. 1991; **104**, 209-25.
[18] CN Davies. Separation of airborne dust and particles. *Proc. Inst. Mech. Eng.* 1952; **1B**, 185-98.

[19] FO Griffin and A Meisen. Impaction of spherical particles on cylinders at moderate Reynolds numbers. *Chem. Eng. Sci.* 1973; **28**, 2155-64.
[20] RC Brown. A many-fiber theory of airflow through a fibrous filter-II: fluid inertia and fiber proximity. *J. Aerosol Sci.* 1986; **17**, 685-97.
[21] N Rao and M Faghri. Computer modeling of aerosol filtration by fibrous filter. *Aerosol Sci. Tech.* 1988; **8**, 133-56.
[22] PC Raynor. Single fiber interception efficiency for elliptical fibers. *Aerosol Sci. Tech.* 2008; **42**, 357-68.
[23] S Chen, CS Cheung, CK Chan and C Zhu. Numerical solution of aerosol collection in filters with staggered parallel rectangular fibers. *Comput. Mech.* 2012; **28**, 152-61.
[24] OY Ming and BYH Liu. Analytical solution of flow field and pressure drop for filters with rectangular fibers. *J. Aerosol Sci.* 1998; **29**, 187-96.
[25] C Zhu, CH Lin and CS Cheung. Inertial impaction dominated fibrous filtration with rectangular or cylindrical fibers. *Powder Tech.* 2000; **112**, 149-62.
[26] H Schlichting. *Boundary Layer Theory*. 6th ed. McGraw-Hill, New York, 1968.
[27] H Lamb. *Hydrodynamics*. 6th ed. Dover Publications, New York, 1945.
[28] SV Patankar, CH Liu and EM Sparrow. Fully developed flow and heat transfer in ducts having streamwise-periodic variations of cross-sectional area. *J. Heat Tran.* 1977; **99**, 180-6.
[29] CN Davies and CV Peetz. Impingement of particles on a transverse cylinder. *Proc. Roy. Soc.* 1956; **234**, 269-95.
[30] JA Harrop and JIT Stenhouse. The theoretical prediction of inertial impaction efficiency in fibrous filters. *Chem. Eng. Sci.* 1969; **24**, 1475-81.